

33. Sequences have been deposited in GenBank, accession numbers L26366 to L26392.
34. B. Bremer, *Plant Syst. Evol.* **175**, 39 (1991).
35. T. E. Dowling, C. Moritz, J. D. Palmer, in (2), pp. 250–317.
36. Sequences were obtained from genes 0.3 (519 nucleotides), 17 and 17.5 (356 nucleotides), and 18 (216 nucleotides). Protein 0.3 inactivates host restriction, protein 17 is a tail fiber protein, and protein 18 functions in DNA maturation. The function of protein 17.5 is unknown.
37. J. Felsenstein, *J. Mol. Evol.* **17**, 368 (1981); *Evolution* **46**, 159 (1992), as implemented in Phylip (27).
38. N. Saitou and M. Nei, *Mol. Biol. Evol.* **4**, 406 (1987).
39. W. M. Fitch and E. Margoliash, *Science* **155**, 279 (1967).
40. R. R. Sokal and C. D. Michener, *Univ. Kans. Sci. Bull.* **38**, 1409 (1958).
41. D. M. Hillis and J. P. Huelsenbeck, *J. Hered.* **83**, 189 (1992).
42. J. Felsenstein, *Biol. J. Linn. Soc.* **16**, 183 (1981); W. C. Wheeler, *Cladistics* **6**, 269 (1990).
43. J. Felsenstein and E. Sober, *Syst. Zool.* **35**, 617 (1986); B. Golding and J. Felsenstein, *J. Mol. Evol.* **31**, 511 (1990); N. Goldman, *Syst. Zool.* **39**, 345 (1990); *J. Mol. Evol.* **36**, 182 (1993).
44. Formulas for calculating the number of possible trees were derived by L. L. Cavalli-Sforza and A. W. F. Edwards [*Evolution* **21**, 550 (1967)]. The actual number of possible phylogenies of life would also have to include trees with reticulations and multifurcations and would need to include all the extinct species that have ever existed, so the estimate shown is conservative.
45. D. L. Swofford and G. J. Olsen, in (2), pp. 411–501.

46. W. D. Hillis and B. M. Boghosian, *Science* **261**, 856 (1993).
47. Figure 3 was based on a reanalysis of the data from (4), by use of uniformly weighted parsimony and TBR branch-swapping with PAUP (27). The tree shown is one of eight equally parsimonious trees of 281 steps (consistency index = 0.68), which differ in minor rearrangements within the dental clade. The local control consensus sequence from the original study was not included because it does not represent an observed sequence.
48. Supported by NSF grants BSR 9106746 and DEB 9221052. We thank B. Bowman, J. J. Bull, C. A. Ciesielski, E. Holmes, H. Jaffe, C. Jenkins, M. Kalish, P. MacManus, I. J. Molineux, G. Myers, G. Schochetman, and D. L. Swofford for advice and assistance.

## RESEARCH ARTICLE

# Genetic Control of Programmed Cell Death in *Drosophila*

Kristin White,\*† Megan E. Grether,\* John M. Abrams,\*‡  
Lynn Young,§ Kim Farrell, Hermann Steller||

A gene, *reaper* (*rpr*), that appears to play a central control function for the initiation of programmed cell death (apoptosis) in *Drosophila* was identified. Virtually all programmed cell death that normally occurs during *Drosophila* embryogenesis was blocked in embryos homozygous for a small deletion that includes the *reaper* gene. Mutant embryos contained many extra cells and failed to hatch, but many other aspects of development appeared quite normal. Deletions that include *reaper* also protected embryos from apoptosis caused by x-irradiation and developmental defects. However, high doses of x-rays induced some apoptosis in mutant embryos, and the resulting corpses were phagocytosed by macrophages. These data suggest that the basic cell death program is intact although it was not activated in mutant embryos. The DNA encompassed by the deletion was cloned and the *reaper* gene was identified on the basis of the ability of cloned DNA to restore apoptosis to cell death defective embryos in germ line transformation experiments. The *reaper* gene appears to encode a small peptide that shows no homology to known proteins, and *reaper* messenger RNA is expressed in cells destined to undergo apoptosis.

Development and homeostasis of most multicellular organisms are critically dependent on mitosis, differentiation, and cell death. In many organisms, a large number of cells die even in the absence of obvious external insults. For example, in vertebrates approximately half of the neurons generated during neurogenesis are eliminated by cell death (1). This deliberate elimi-

nation of cells occurs in a morphologically distinct manner and is referred to as apoptosis or programmed cell death; it is distinct from cell death provoked by external injury (2). Because apoptosis often requires RNA and protein synthesis, it is thought that it results from active, gene-directed processes (3). However, except in the nematode *Caenorhabditis elegans*, no genes have been identified that are globally required for this process (4).

The many genetic techniques available for studying *Drosophila* make it an ideal model system in which to dissect the genetic control of programmed cell death and its role in development. Cell death occurs during the course of *Drosophila* development by apoptosis (5, 6). The onset of death is dependent on hormonal cues in some cases and on cell-cell interactions in others (7, 8). These types of interactions

demonstrate that cell death in *Drosophila*, like that in vertebrates, is under epigenetic control.

In order to identify genes that are required for programmed cell death in *Drosophila*, we examined the pattern of cell death in embryos homozygous for chromosomal deletions. Because more than 50 percent of the *Drosophila* genome is represented by such deletion strains, we were able to rapidly screen a substantial fraction of the genome for cell death genes (9). Although these deletions typically include genes essential for viability, the large maternal supply of nutrients, protein, and RNA (10) permits development well beyond the stage at which cell death begins.

In the wild-type embryo, a substantial amount of apoptotic cell death occurs in a relatively predictable pattern (6). These deaths can be rapidly and reliably detected in live embryos by staining with vital dyes, such as acridine orange (AO). These preparations allow an assessment of the effect of mutations on cell death in many different tissues, and the subsequent identification of genes that are globally required for programmed cell death.

Among the 129 deletion strains examined, the majority (83 strains, 65 percent) did not appreciably affect the extent to which cell death occurred in the embryo. Among the remaining deletion strains, approximately 20 percent resulted in excessive cell death, and some (13 percent) showed a decrease in the number of AO staining cells. Of all the strains examined, only three overlapping deletions, *Df(3L)WR4*, *Df(3L)WR10*, and *Df(3L)Cat<sup>DH104</sup>* (11, 12), produced embryos that lacked all AO staining (less than 1 percent of wild-type amounts) at all stages of development (Fig. 1, A and B). These deletions overlap in genomic region 75C1,2 on the third chromosome. We subsequently obtained another mutation in this region, *hid<sup>H99</sup>* (*H99*) (13), that showed the same phenotype. Although this mutation appears cytologically normal, molecular analysis revealed that *H99* is also a deletion that is internal to the overlap of the

The authors are in the Howard Hughes Medical Institute, Department of Brain and Cognitive Sciences and Department of Biology, Massachusetts Institute of Technology, Cambridge, MA 02139, USA.

\*These authors contributed equally to this study.

†Present address: Cutaneous Biology Research Center, Massachusetts General Hospital, Harvard Medical School, Charlestown, MA 02129, USA.

‡Present address: Department of Cell Biology and Neuroscience, University of Texas Southwestern Medical Center, Dallas, TX 75235, USA.

§Present address: Whitehead Institute for Biomedical Research, Cambridge, MA 02142, USA.

||To whom correspondence should be addressed.

deficiencies *Df(3L)WR4*, *Df(3L)WR10*, and *Df(3L)Cat<sup>DH104</sup>* (data provided below).

To demonstrate that the lack of AO staining in *H99* embryos reflected the absence of cell death, we analyzed tissue

sections by transmission electron microscopy (Fig. 1, C and D). In wild type, many apoptotic cells were visible in all sections from embryos older than stage 12. In contrast, no features characteristic of apoptosis

were detected in homozygous *H99* embryos at any developmental stage. We conclude that programmed cell death does not occur in these mutants.

We considered the possibility that the lack of cell death in *H99* embryos was the result of a general block in development that was caused by the absence of functionally unrelated genes. Several observations led us to conclude that this is unlikely. (i) Mutant embryos reached advanced developmental stages. They formed a segmented cuticle and began to move, but failed to hatch. In addition, mutant embryos expressed markers that are only present in differentiated cells. (ii) In a survey of more than 129 deletions (approximately 50 percent of the genome), only those in chromosomal region 75C1,2 resulted in the complete absence of all programmed cell deaths. Many other deletions caused severe developmental defects, yet none completely blocked programmed cell death. (iii) Furthermore, mitotic clones of *H99* in the eye contained fully differentiated and morphologically normal photoreceptor neurons (14). This demonstrates that the *H99* deletion does not have adverse effects on cell division, differentiation, or survival. (iv) Finally, as shown below, apoptosis could be induced in *H99* embryos upon x-irradiation. These results suggest that a general, nonspecific cellular defect, for example, in energy metabolism or protein synthesis, is not the underlying cause for the observed phenotype.

**Developmental defects in cell death defective embryos.** The absence of cell death

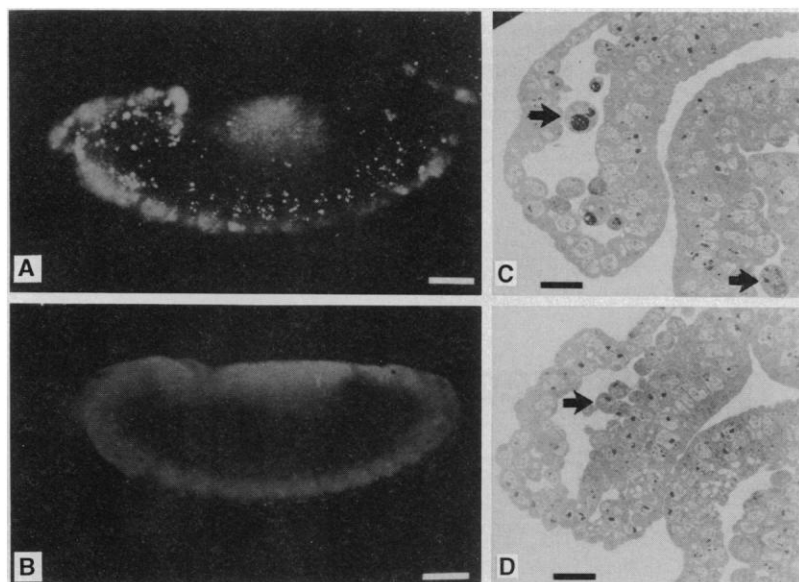


**Fig. 1.** Embryos deleted at 75C1,2 lack almost all apoptotic cell death. Deletion stocks were screened for cell death by AO staining (9). (A) Wild-type embryo stained with AO. (B) Homozygous *Df(3L)WR4* embryo of the same age stained with AO. Scale bars in (A) and (B) are 50  $\mu$ m. (C) Electron micrograph of the clypeolabrum of a wild-type embryo. Electron dense cell corpses that have been engulfed by macrophages are indicated by the arrow. Embryos were fixed and sectioned for electron microscopy as described (6). (D) Clypeolabrum of homozygous *H99* embryo. Mutant embryos were identified on the basis of their AO phenotype prior to fixation. The circulating cells within the subepidermal spaces of both wild-type and mutant embryos (arrow) are macrophages; they express macrophage-specific markers (6). In mutant embryos, these cells are smaller than in wild type because they lack apoptotic corpses. Scale bars in (C) and (D) are 10  $\mu$ m.

**Fig. 2.** Embryos that lack cell death have extra cells. (A) Central nervous system of wild-type embryo stained with antibody to *elf-1* (36). The antibody staining was imaged on a confocal microscope, and a series of images were summed to give a complete picture of the staining throughout the ventral cord. The arrows in (A) and (B) mark the approximate boundary between the thoracic and abdominal neuromeres. Approximately six cells stain in each abdominal neuromere. (B) Central nervous system of a fully developed *H99* homozygous embryo. These embryos are easily distinguished from their heterozygous siblings by the abnormal cephalopharyngeal skeleton (13). Mutant embryos contain more than 20 cells in some of the abdominal neuromeres. Scale bars in (A) and (B) are 10  $\mu$ m. (C) Staining of antibody to Kr (anti-Kr) of a stage 16 wild-type embryo (37). At this stage, the anti-Kr stains a subset of cells in the central nervous system, as well as cells in the larval photoreceptor organ (arrow) (18). (D) Anti-Kr staining of a stage 16 homozygous *H99* embryo. There are many more Kr-positive cells in the central nervous system of mutant embryos. There also appear to be more cells in the larval photoreceptor organ (arrow). Scale bars in (C) and (D) are 50  $\mu$ m. (E) Higher magnification of the ventral cord of a wild-type embryo stained with the Kr antibody. (F) Kr antibody staining of the ventral cord of a homozygous *H99* embryo of a similar age. An increased number of cells stain with the Kr antibody in the *H99* embryo. Scale bars in (E) and (F) are 20  $\mu$ m.

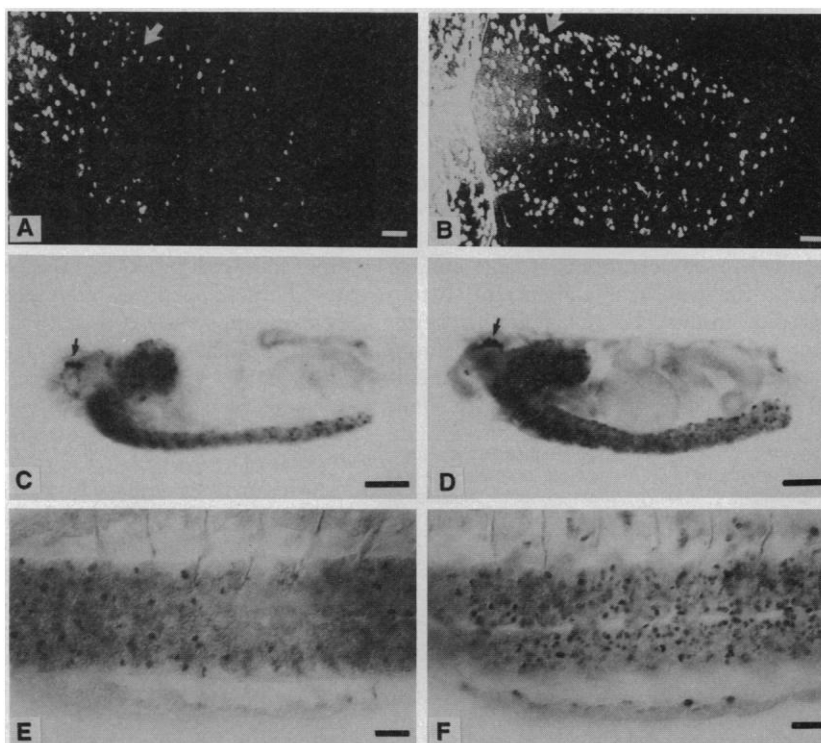
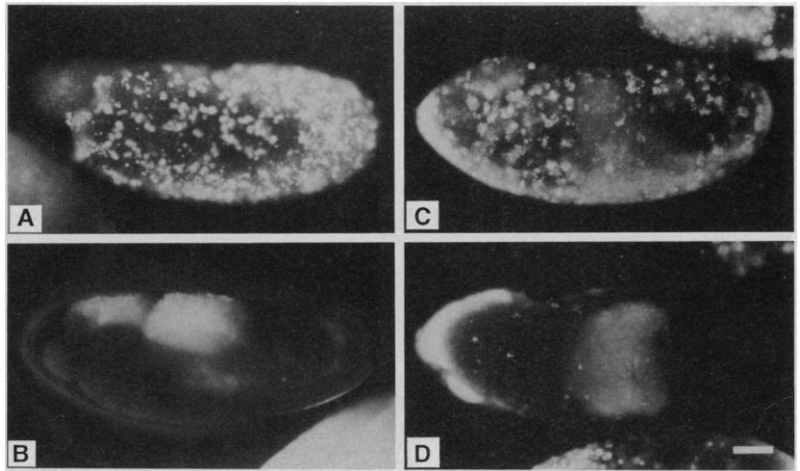


**Fig. 3.** Cell death defective deletions protect against ectopic cell death. Cell death was visualized in these experiments by AO staining. (A) Embryos homozygous for the mutation *crumbs* display massive amounts of ectopic cell death. (B) Mutant embryo that is homozygous for both *crumbs* and *Df(3L)WR10*. The deletion completely blocks cell death in most double mutant embryos. X-irradiation also induces ectopic apoptosis in *Drosophila* embryos. (C) Wild-type embryo irradiated with 4000 rad and aged for 10 hours (38). (D) *Df(3L)WR4/Df(3L)WR10* embryo treated in the same manner. The mutant embryo has many fewer staining cells than the wild-type embryo. At lower doses of radiation (~500 rad) excess staining was induced in wild-type embryos, but only very little or none in mutant embryos. Scale bar is 50  $\mu$ m.



in mutant embryos is expected to result in the presence of extra cells. This prediction was tested by counting specific cells in the central nervous system, a tissue subject to extensive cell death during wild-type development (6). One cell type that normally undergoes programmed death in insects is the abdominal neuroblast (15). In *Drosophila*, approximately 25 cells are born in each abdominal neuromere, but only six cells persist to eventually produce neurons in the imaginal ganglia (16). Using the *elf-1* antibody to visualize these cells (17), we found that their number was greatly increased in mutant embryos (Fig. 2, A and B). Whereas approximately six cells stain in each abdominal neuromere in the wild-type nervous system (Fig. 2A), 20 or more cells stain in some of the abdominal segments of the mutant nervous system (Fig. 2B). This result demonstrates that supernumerary neuroblasts are present in fully developed *H99* embryos, and confirms our expectations that a block of cell death should lead to an increase in the number of these cells.

We also used an antibody to the Krüppel (Kr) protein to label a subset of cells in the late embryonic central nervous system (18). In mutant embryos, the overall size of the central nervous system was substantially increased (Fig. 2, C and D). Cell counts revealed that this antibody stained two to three times as many cells in the ventral nerve cord of mutant embryos of identical age. For example, the number of Kr-positive cells in three neuromeres ranged from 159 to 189 in wild-type embryos, as opposed to 364 to 445 in the same neuromeres of homozygous *H99* embryos (compare Fig. 2, C and E to D and F). Finally, there appeared to be a similar increase in the number of cells in the larval photoreceptor organ (Fig. 2, C and D). These experiments demonstrate that many extra cells are present in the nervous system of mutant embryos and suggest that at least half of the cells in the wild-type nervous system

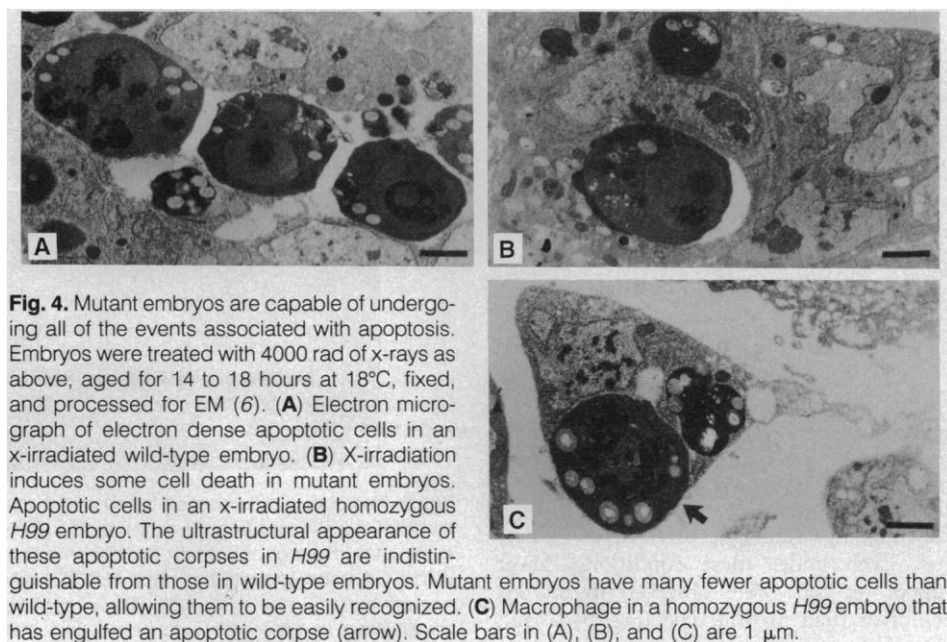
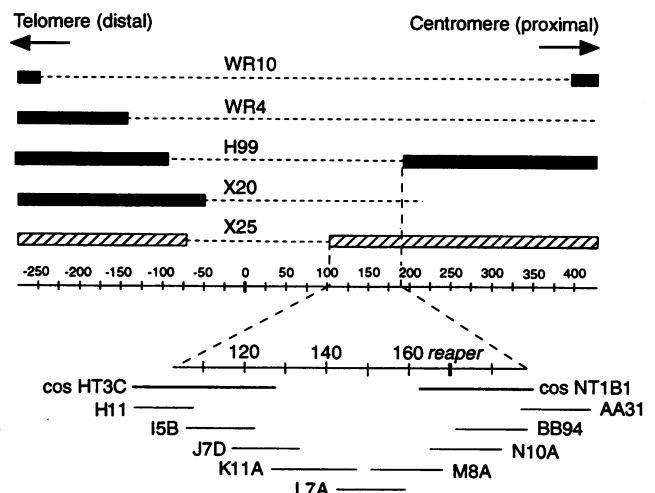


**Fig. 4.** Mutant embryos are capable of undergoing all of the events associated with apoptosis. Embryos were treated with 4000 rad of x-rays as above, aged for 14 to 18 hours at 18°C, fixed, and processed for EM (6). (A) Electron micrograph of electron dense apoptotic cells in an x-irradiated wild-type embryo. (B) X-irradiation induces some cell death in mutant embryos. Apoptotic cells in an x-irradiated homozygous *H99* embryo. The ultrastructural appearance of these apoptotic corpses in *H99* are indistinguishable from those in wild-type embryos. Mutant embryos have many fewer apoptotic cells than wild-type, allowing them to be easily recognized. (C) Macrophage in a homozygous *H99* embryo that has engulfed an apoptotic corpse (arrow). Scale bars in (A), (B), and (C) are 1  $\mu$ m.

**Fig. 5.** Genetic and molecular map of the 75C1,2 region. The depicted deletions (39) define an 85-kb interval that contains at least a portion of a cell death gene. Dotted lines represent deleted DNA, and the scale represents kilobases of cloned DNA; the position of relevant clones is also indicated (40, 41). Embryos homozygous for deletions *WR10*, *WR4*, *H99*, and *X20* all show the full cell death defective phenotype. In contrast, apoptosis in *X25* embryos is essentially normal, although it is detectably reduced in embryos of the genotype *X25/H99*. This indicates that an 85-kb interval between the proximal breakpoints of *X25* and *H99* must be deleted to give the full cell death defective phenotype. By Northern analysis, only a single transcription unit, *reaper*, has been detected in this region. The cosmid NT1B1, which encompasses this transcription unit, was used to generate transgenic flies.



are eliminated by programmed cell death.

A large number of developmental mutations in *Drosophila* lead to ectopic cell death (6, 19–22). We were interested in determining whether the cell death function in the 75C1,2 interval was required for such ectopic deaths. The *crumbs* mutation leads to widespread defects in the development of the epithelial tissues, followed by massive cell death during embryogenesis (21) (Fig. 3A). We found that *Df(3L)WR10* blocks the massive ectopic death seen in *crumbs* mutant embryos. Virtually no AO staining was observed in most double mutant embryos (Fig. 3B), indicating that normal and ectopic cell deaths involve a common pathway. The gross morphological defects caused by the *crumbs* mutation are not rescued by the block in cell death. These data indicate that deletions in 75C1,2 can be used as a general tool for blocking cell death. Therefore, it should now be possible to critically assess the role of cell death in the context of both normal and mutant development.

**The basic cell death program is intact in *H99* embryos.** We also examined the possible induction of cell death in *H99* embryos by x-irradiation. Ionizing radiation induces apoptosis in both mammalian cells (23, 24) and *Drosophila* wild-type embryos (6), but appears to involve a signaling mechanism that is distinct from those controlling developmental cell deaths (24). At low doses of x-irradiation (~500 rad), *H99* embryos were resistant to x-ray induced cell death. However, higher doses were capable of inducing some apoptosis in *H99* embryos. Even under these conditions, fewer apoptotic cells were observed in mutant embryos than in wild type (Fig. 3, C and D). Therefore, this mutation provides some protection against radiation-induced cell death. However, the morphology of apoptotic cells in irradiated *H99* embryos was indistinguishable from that in the wild type (Fig. 4, A and B). Cells in mutant embryos thus can undergo apoptosis, even though they do not do so during normal development. Furthermore, apoptotic cells in mutant embryos become targets for engulfment by macrophages (Fig. 4C). We conclude that the defect in *H99* embryos lies upstream of the terminal cellular events of apoptosis. Once induced, the cell death program can apparently be executed in mutant embryos and, as in the wild type, apoptotic corpses can be recognized and phagocytosed by macrophages. Taken together, our results indicate that *H99* deletes a function of central importance for the initiation of programmed cell death in *Drosophila*.

The function deleted by *H99* could either affect the process by which cells are selected to die, or the initiation of the cell death program within selected cells. The

former possibility appears to be less likely because it would require that cells be selected to die with a single ubiquitous signal. A large number of cells undergo apoptosis during *Drosophila* embryogenesis, and these cells are localized in a variety of different places and they die at multiple developmental stages. The onset of some cell deaths appears to be dependent on cell-cell interactions, whereas other cell deaths may be determined by cell lineage (6, 15, 22, 25). Because of the different circumstances under which cell death can occur, it seems

unlikely that all such deaths could be induced by a common signal. Indeed, a number of mutations have been identified in *Drosophila* that affect cell death in particular tissues (7, 8, 19–22). These mutations may influence cell death by affecting a tissue-specific signaling event, or by more generally altering the cellular environment. In contrast, the *H99* mutant appears to globally block the initiation of apoptosis. In this regard, it is similar to the *ced-3* and *ced-4* mutations that prevent the onset of all programmed

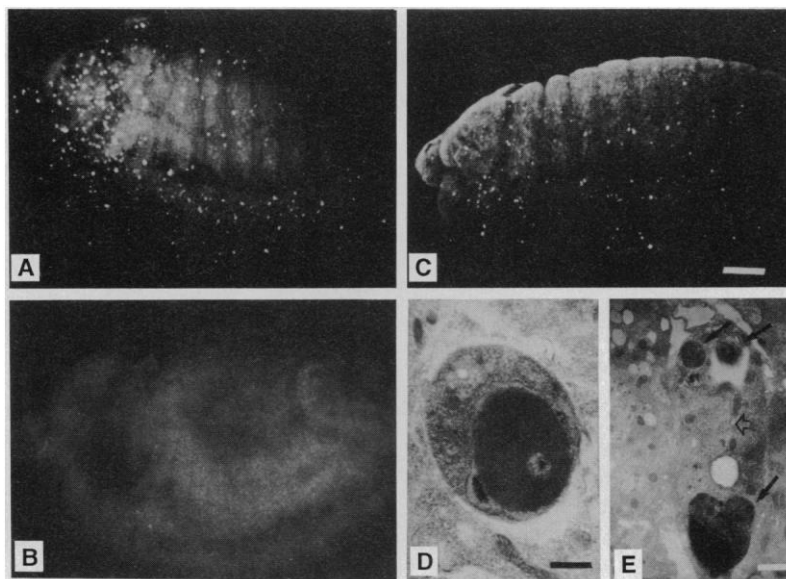


**Fig. 6.** Restoration of apoptosis by cosmid transformation. Cosmid clone NT1B1, which contains the *rpr* transcription unit (Fig. 5) was used to generate transgenic flies (41). This transgene restored significant levels of cell death to *H99* embryos, as assayed by AO and TUNEL, shown here. (A) Wild-type embryo labeled with the TUNEL technique (42). Each of the bright spots represents the nuclear material of a dying cell. (B) An *H99* mutant embryo labeled with TUNEL. There is virtually no staining in *H99* embryos, confirming that even early events in apoptosis, such as DNA degradation, do not occur. (C) An *H99* mutant embryo that carries four copies of the NT1B1 cosmid transgene. This construct restored significant amount of cell death to *H99* embryos, although not to that in wild-type. Scale bars are 50  $\mu$ m for (A), (B), and (C). Electron microscopy (6) was used to confirm the apoptotic nature of cell deaths in transgenic embryos. (D) An apoptotic cell in an *H99* embryo containing two copies of the NT1B1 transgene. The scale bar is 0.4  $\mu$ m. (E) A macrophage in the same embryo that has engulfed several apoptotic corpses (black arrows). The open arrow indicates the macrophage nucleus. The scale bar is 1.4  $\mu$ m.

**Fig. 7.** Predicted amino acid sequence of *reaper*. The nucleotide sequence of the longest open reading frame found in the *rpr* cDNA is shown on the top line. The full cDNA sequence can be accessed from Genbank (accession number L31631). On the second line is the homologous sequence from *D. simulans* (43). We found 5 base changes within 94 base pairs of reliable sequence, none of which change the amino acid translation of this ORF. The conceptual translation, shown below the DNA sequence, gives rise to a peptide of 65 amino acids.

```

10          30          50
ATGGCAGTGGCATTCTACATACCCGATCAGGCGACTCTGTTCGGGAGGCGGAGCAGAAG
                                     |||||
M A V A F Y I P D Q A T L L R E A E Q K
70          90          110
GAGCAGCAGATTCTCCGCTTGGGGAGTCACAGTGGAGATTCTGGCCACCGTCGTCCTG
|||||
GAGCAGCAGATCTCCGCTTGGGGAGTCCAGTGGAGATTCTGGCCACCGTTGTCCTG
      C          C          T
E Q Q I L R L R E S Q W R F L A T V V L
130          150          170
GAAACCTGCGCCAGTACAATTCTATGTCATCCGAAGACCGGAAGAAAGTCCGGCAAATAT
|||||
GAAACGCTGGCCACT
      G          C
E T L R Q Y T S C H P K T G R K S G K Y
190
CGCAAGCCATCGCAATGA
R K P S Q *

```

cell deaths in the nematode *C. elegans* (26).

**Isolation and molecular characterization of *reaper*.** In spite of considerable effort, we have been unable to generate any single gene mutations in the *H99* interval that substantially affect the pattern of em-

bryonic cell death (27). The cell death gene may be relatively resistant to chemical mutagens, or the cell death function may be encoded by two or more functionally redundant genes within the *H99* interval.

To identify a cell death gene within the

*H99* deletion, we cloned all of the DNA within this interval. By generating additional breakpoints with x-ray mutagenesis we were able to map at least a portion of a cell death gene to an 85-kb interval (Fig. 5). Next, we tested the ability of cosmid clones from this region to restore apoptosis to *H99* embryos. Cosmid NT1B1 was capable of restoring apoptosis to transgenic *H99* embryos, although not to wild-type levels (Fig. 6). In contrast, other transgenes failed to restore apoptosis to *H99* embryos (28). These results suggest that a cell death gene is localized within NT1B1. This clone appears to contain only a single transcription unit, which we have named *reaper* (*rpr*). In situ hybridization analysis indicates that *rpr* expression from the transgene is indistinguishable from expression of the endogenous gene. However, we cannot rule out defects in posttranscriptional expression or in the activity of the product as the cause of the partial rescue. Expression of a *reaper* complementary DNA (cDNA) (described below) under the heat-inducible *hsp70* promoter is sufficient to induce extensive apoptosis in transgenic *H99* embryos (14), confirming that *reaper* is indeed responsible for the activity of the cosmid transgene.

The *reaper* gene appears to encode a single polyadenylated transcript of approximately 1300 bp (29). We have isolated and sequenced two independent cDNA clones from a  $\lambda$ gt-10 eye disc library (30). Both cDNAs appear to be truncated at the 5' end, but the longer clone (13B2) is biologically active, as demonstrated by its ability to restore cell death in *H99* embryos. The 5' most ATG in these cDNAs is followed by an open reading frame (ORF) of 65 amino acids (Fig. 7). The sequence preceding this ATG is in good agreement with the consensus for translation initiation (31), and the codon usage of this ORF is typical for *Drosophila* proteins. The deduced *reaper* peptide sequence does not show any large degree of similarity to other protein sequences presently in the database. Although this ORF is extremely small, it appears to be biologically relevant. We have used polymerase chain reaction to isolate homologous DNA segments from other *Drosophila* species. Comparison of a 94-bp segment of the *rpr* ORF from *Drosophila melanogaster* and *Drosophila simulans* revealed five nucleotide changes. All of these changes were in the third codon position and did not alter the predicted amino acid sequence of the protein (Fig. 7). This suggests that there is selective pressure to conserve this sequence as a protein coding region. The small size of this ORF might explain our difficulty in generating a point mutation that eliminated cell death. However, these data do not rule out the possible existence of another cell death gene within the *H99* interval.

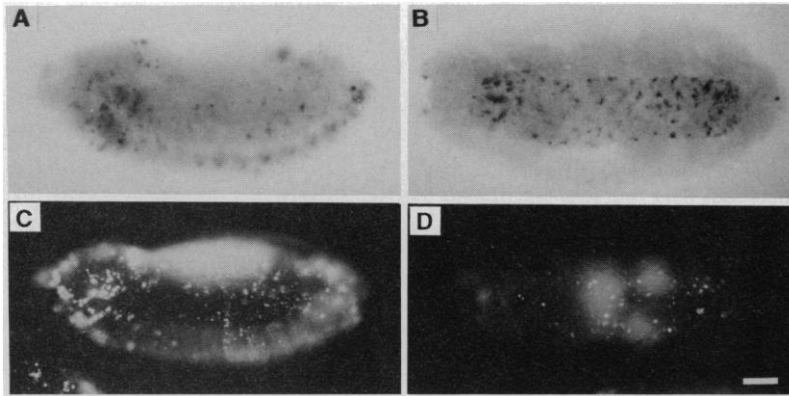


**Fig. 8.** Expression of the *reaper* gene corresponds to the pattern of programmed cell death in the *Drosophila* embryo. Single-stranded RNA probes for *rpr* were used for in situ hybridization to whole mount embryos (A and B) (44). Panels (C) and (D) show corresponding patterns of AO staining in slightly older embryos. The *rpr* transcript is present in precisely the same regions of the embryo in which cell death will later occur, for example in the dorsal head, gnathal segments, and scattered cells in the abdominal segments of the stage 13 to 14 embryos (A and C). The diffuse staining is the result of autofluorescence of the yolk. In older embryos both *rpr* transcription and AO staining are almost entirely restricted to cells in the central nervous system (B and D). Because *rpr* expression precedes apoptosis by 1 to 2 hours, AO stained embryos are shown here at slightly more advanced developmental stages. For example, the CNS of the embryo in (D) is more condensed than that shown in (B). Scale bars are 45  $\mu$ m.

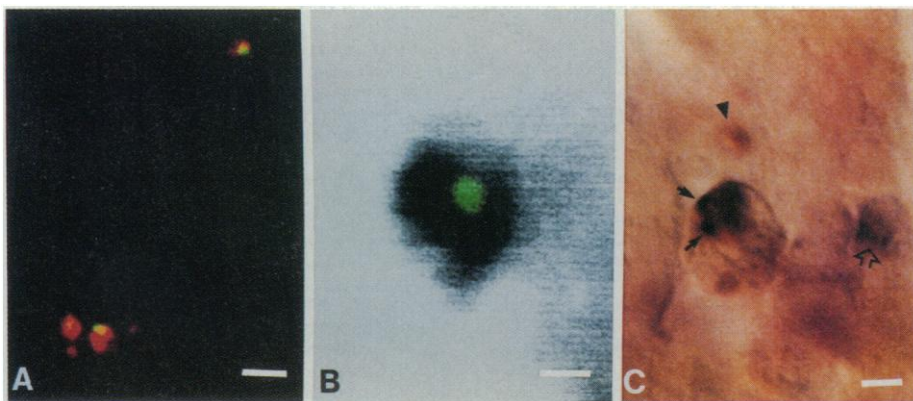
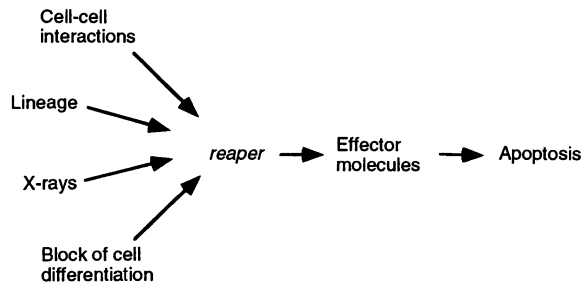


**Fig. 9.** Expression of *reaper* in dying cells. Double labeling for *rpr* and TUNEL was used to determine whether *rpr* is expressed in dying cells or their neighbors. Visualization of cell death by TUNEL was with either fluorescent or histochemical detection methods, and expression of *rpr* was detected by in situ hybridization (45). These experiments demonstrate that, for a given timepoint, TUNEL and *rpr* label an overlapping but not identical set of cells. Expression of *rpr* precedes cell death as assayed by TUNEL, and TUNEL appears to persist longer in the dying cells. (A) Several cells that are double labeled with TUNEL (red) and *rpr* (green). Expression of *rpr* often appears as a small crescent around the TUNEL stained nucleus, perhaps as a result of the condensation of the cytoplasm in the dying cell. Scale bar is 5  $\mu$ m. (B) The nucleus of a single large apoptotic cell (green TUNEL staining) is surrounded by *rpr* labeled cytoplasm, demonstrating that *rpr* is expressed in the dying cell itself. Scale bar is 2.5  $\mu$ m. (C) A macrophage contains a cell that is double-labeled for *rpr* and TUNEL, demonstrating that *rpr* is expressed in cells that die and become engulfed by macrophages. In this experiment, *rpr* expression produced black staining and TUNEL, brown staining. The *rpr* labeled cell within the macrophage is marked by black arrows. Examination at different focal planes revealed that the nucleus of this cell was TUNEL-positive, even though this is difficult to appreciate in this picture. Two other cells visible in this photograph are positive only for *rpr* (open arrow) or TUNEL (black arrowhead). We believe that these represent very early (*rpr*-positive) and very late (TUNEL-positive) stages of apoptosis, respectively. Scale bar in C is 2  $\mu$ m.

**Fig. 10.** Model for the role of *reaper* in programmed cell death. We propose that the expression of the *rpr* gene serves as a global and central switch point between life and death. Cell death in *Drosophila* is controlled by a number of distinct signals, including various extracellular signals (7, 8, 22), internal signals such as lineage (15, 25), the arrest of cellular differentiation (6, 20, 21), and x-ray-induced damage (6, 23, 24). The *H99* deletion protects against apoptosis induced by these diverse types of signals, indicating that the initiation of all these deaths involves a common pathway in which *reaper* is of pivotal importance. Further support for this idea comes from the observation that ectopic *rpr* expression is induced upon treatments that cause ectopic cell death, such as x-irradiation (46). Our model also predicts that *rpr* acts upstream of cell death effectors to initiate apoptosis.



In the *Drosophila* embryo, *reaper* RNA is expressed in a pattern that is very similar to the pattern of programmed cell death (Fig. 8). The onset of *rpr* expression typically precedes AO staining by 1 to 2 hours. In double labeling experiments the TUNEL technique (32) was used to mark dying cells. This method utilizes terminal transferase to incorporate biotinylated nucleotides at the end of DNA double-strand breaks, thereby permitting the in situ detection of apoptotic nuclei that contain fragmented DNA. These experiments demonstrate that the *rpr* transcript is expressed in the dying cells themselves (Fig. 9). This is also supported by the presence of *rpr* RNA in phagocytosed corpses within macrophages (Fig. 9C). Because this transcript appears to be specifically expressed in cells that will later die, it should be a useful marker for the identification of doomed cells before there is any morphological manifestation of apoptosis.

Our results demonstrate that virtually all programmed cell deaths that occur during *Drosophila* embryogenesis are under genetic control. In spite of the considerable morphological and developmental diversity of cell deaths seen in this organism, the initiation of all these deaths appears to involve a common pathway. We propose that *reaper* plays a central and global regulatory function for the initiation of apoptosis (Fig. 10). We believe that *reaper* is not part of the cell death effector machinery itself, because the few cells that die upon x-irradiation in mutant embryos display all the morphological characteristics of apoptosis, indicating that the basic cell death program is still in place. According to our model, *reaper* would activate cell death effectors that may be present in most, if not all cells (33). This could occur by either directly activating cell death effector molecules, or by inhibiting negative regulators of cell death, such as *bcl-2* (34). We expect that the biochemical characterization of *rpr*, and the identification of genes with which it interacts, should provide further insight

into the molecular basis of programmed cell death in *Drosophila*, and possibly in other organisms as well.

## REFERENCES AND NOTES

- V. Hamburger, *J. Comp. Neurol.* **160**, 535 (1975); W. M. Cowan, J. W. Fawcett, D. D. M. O'Leary, B. B. Stanfield, *Science* **225**, 1258 (1984); R. W. Oppenheim, *Annu. Rev. Neurosci.* **14**, 453 (1991).
- J. F. R. Kerr, A. H. Wyllie, A. R. Currie, *Br. J. Cancer* **26**, 239 (1972).
- J. R. Tata, *Dev. Biol.* **13**, 77 (1966); R. A. Lockshin, *J. Insect Physiol.* **15**, 1505 (1969); D. P. Martin *et al.*, *J. Cell Biol.* **106**, 829 (1988); R. W. Oppenheim, D. Prevette, M. Tytell, S. Homma, *Dev. Biol.* **138**, 104 (1990); L. M. Schwartz, L. Kosz, B. K. Kay, *Proc. Natl. Acad. Sci. U.S.A.* **87**, 6594 (1990); B. A. Barres *et al.*, *Cell* **70**, 31 (1992).
- R. E. Ellis, J. Yuan, J. H. R. Horvitz, *Annu. Rev. Cell Biol.* **7**, 663 (1991); R. S. Freeman, S. Estus, K. Horigome, E. M. Johnson Jr., *Curr. Opin. Neurobiol.* **3**, 25 (1993).
- F. Giorgi and P. Deri, *J. Embryol. Exp. Morphol.* **35**, 521 (1976).
- J. M. Abrams, K. White, L. I. Fessler, H. Steller, *Development* **117**, 29 (1993).
- K.-F. Fischbach and G. Technau, *Dev. Biol.* **104**, 219 (1984); H. Steller, K.-F. Fischbach, G. M. Rubin, *Cell* **50**, 1139 (1987); R. L. Cagan and D. F. Ready, *Genes Dev.* **3**, 1099 (1989); K. Kimura and J. W. Truman, *J. Neurosci.* **10**, 403 (1990); A. R. Campos, K.-F. Fischbach, H. Steller, *Development* **114**, 355 (1992).
- T. Wolff and D. F. Ready, *Development* **113**, 825 (1991).
- Deletion strains were obtained from the Bloomington stock center, Bloomington, IN. Embryos were collected for 6 hours at 25°C, aged for an additional 16 hours at 18°C, and stained for AO (6).
- A. Garcia-Bellido, J. Moscoso del Prado, J. Botas, *Mol. Gen. Genet.* **192**, 253 (1983).
- W. A. Segraves and D. S. Hogness, *Genes Dev.* **4**, 204 (1990).
- W. J. Mackay and G. C. Bewley, *Genetics* **122**, 643 (1989).
- M. K. Abbott and J. A. Lengyel, *ibid.* **129**, 783 (1991).
- K. White and H. Steller, unpublished data.
- C. M. Bate, *J. Embryol. Exp. Morphol.* **35**, 107 (1976).
- J. Campos-Ortega and V. Hartenstein, *The Embryonic Development of Drosophila Melanogaster* (Springer-Verlag, New York, 1985); J. W. Truman and M. Bate, *Dev. Biol.* **125**, 145 (1988); A. Prokop and G. M. Technau, *Development* **111**, 79 (1991).
- S. J. Bray, B. Burke, N. H. Brown, J. Hirsh, *Genes Dev.* **3**, 1130 (1989); J. W. Truman, personal communication.
- U. Gaul, E. Seifert, R. Schuh, H. Jäckle, *Cell* **50**, 639 (1987).

- D. Fristrom, *Mol. Gen. Genetics* **103**, 363 (1969); C. Murphy, *Dev. Biol.* **39**, 23 (1974); K.-F. Fischbach and G. Technau, *ibid.* **104**, 219 (1984); A. Martinez-Arias, *J. Embryol. Exp. Morphol.* **87**, 99 (1985); H. Steller, K.-F. Fischbach, G. M. Rubin, *Cell* **50**, 1139 (1987); J. Klingensmith, E. Noll, N. Perrimon, *Dev. Biol.* **134**, 130 (1989).
- N. M. Bonini, W. M. Leiserson, S. Benzer, *Cell* **72**, 379 (1993).
- U. Tepass and E. Knust, *Roux's Arch. Dev. Biol.* **199**, 189 (1990).
- L. Magrassi and P. A. Lawrence, *Development* **104**, 447 (1988).
- C. S. Potten, S. E. Al-Barwari, J. Searle, *Cell Tissue Kinet.* **11**, 149 (1978); S. R. Umansky, in *Apoptosis: The Molecular Basis of Cell Death*, L. D. Tomei and F. O. Cope, Eds. (Cold Spring Harbor, NY, 1991).
- S. W. Lowe, E. M. Schmitt, S. W. Smith, B. A. Osborne, T. Jacks, *Nature* **362**, 847 (1993); A. R. Clarke *et al.*, *ibid.*, p. 849.
- M. Bate, C. S. Goodman, N. C. Spitzer, *J. Neurosci.* **1**, 103 (1981).
- J. Yuan and H. R. Horvitz, *Dev. Biol.* **138**, 33 (1991).
- Several large-scale mutagenesis experiments for both lethal and visible gene mutations have identified only one complementation group, *head involution defective* (*hid*), which maps to the genomic interval (13) (M. Grether, J. Abrams, K. White, L. Young, unpublished observations). Null mutations in *hid* did not show any detectable reduction of AO staining. Cell death defective mutations in *Drosophila* are expected to produce at least a readily detectable rough eye phenotype (8). It is possible that the cell death gene is not very mutable with chemical mutagens, or that the cell death function is encoded by two or more functionally redundant genes within the *H99* interval.
- We also generated germline transformants with another cosmid from the 75C1.2 region (cos HT3C), which overlapped the X25 breakpoint. This cosmid transgene did not result in any detectable increase in the amount of cell death in *H99* embryos. In addition, a transgene containing a *disco* cDNA under the control of the *hsp70* promoter also did not result in detectable increases in cell death in *H99* embryos after heat shock, even though it does cause drastic developmental defects (A. R. Campos, K. Lee, H. Steller, in preparation).
- J. M. Abrams and H. Steller, unpublished observations.
- Two independent cDNA clones were isolated from a lambda gt10 eye disc library (A. Cowman and G. M. Rubin). The cDNA inserts of approximately 860 and 900 bp were subcloned into pBS II SK (Stratagene), and sequenced in both orientations with Sequenase (United States Biochemical). The cDNA sequence was also confirmed by partial genomic sequence analysis.
- M. Kozak, *Nucleic Acids Res.* **12**, 857 (1984); D. R. Casavant, *ibid.* **15**, 1353 (1987).
- Y. Gavrieli, Y. Sherman, S. A. Ben-Sasson, *J. Cell Biol.* **119**, 493 (1992).
- M. C. Raff, *Nature* **356**, 397 (1992); M. C. Raff *et al.*, *Science* **262**, 695 (1993).
- D. L. Vaux, S. Cory, J. M. Adams, *Nature* **335**, 440 (1988); D. Hockenberry, G. Nuñez, C. Millman, R. D. Schreiber, S. J. Korsmeyer, *ibid.* **348**, 334 (1990); T. E. Allsop, S. Wyatt, H. F. Paterson, A. Davies, *Cell* **73**, 295 (1993); G. T. Williams and C. A. Smith, *ibid.* **74**, 777 (1993).
- M. Ashburner, *Drosophila: A Laboratory Manual* (Cold Spring Harbor, NY, 1989).
- For elf-1 antibody staining, the central nervous system was dissected from fully developed wild type and *H99* homozygous embryos. The nervous systems were fixed in 2 percent paraformaldehyde in 0.1 M phosphate buffer for 20 minutes at room temperature. The nervous systems were washed and blocked, and incubated in the elf-1 antibody overnight at 4°C. They were washed and incubated with FITC-conjugated second antibody at 4°C overnight.
- Kr staining was done as described (18).

38. Because the effect of x-irradiation on embryos is known to vary during development [F. E. Würzler and H. Ulrich, in *The Genetics and Biology of Drosophila-1C*, M. Ashburner and E. Novitski, Eds. (Academic Press, New York, 1976)], it was necessary to be sure that the treated embryos were as homogeneous in age as possible. Embryos were collected from *CS* or *Df(3L)WR4/TM3 × Df(3L)WR10/TM6B* crosses and selected at blastoderm stage by morphology. These embryos were then kept under Voltalef oil (Atochem) for 1.5 hours and exposed to 4000 rad in a Torrex 120D x-ray machine.
39. New deletions in the 75C1,2 region were generated by reverting the *Wrinkled* (*W*) mutation, a dominant allele of the *hid* gene (13). Males heterozygous for *W* were x-irradiated (3000 to 4000 rad), and mated to balancer females. Progeny were identified in which *W* had reverted. Lines were tested for viability against the *H99* deletion. Of the 117,000 mutagenized chromosomes screened, four fertile revertants were recovered. Breakpoints of new, and previously identified deletions were mapped by Southern analysis of DNA from embryos homozygous for the deletion, or transheterozygous for the deletion being studied over *H99*. These embryos have a severe head involution defect, and can easily be identified. Embryos were collected overnight and aged for at least 24 hours at 25°C. Embryos were then dechorionated in bleach, and those that had not hatched and had not undergone head involution were selected and frozen for DNA preparation. DNA was prepared as described (35).
40. Phage DNAs were isolated from a library of Canton-S genomic DNA in the lambda dash II vector (Stratagene) provided to us by R. Davis. Genomic walking was initiated from two starting points, clones provided by B. Segraves (11) which extended into the *H99* interval from the distal side, and from the *terminus* transcription unit [R. M. Baldarelli *et al.*, *Dev. Biol.* 125, 85 (1988)]. By PCR we generated a 750-bp fragment corresponding to the genomic *terminus* locus. Phage clones corresponding to this locus were isolated and used as a second starting point to walk into the *H99* interval from the proximal side. Breakpoints of the deletions were identified as described above. Putative transcribed regions were identified by reverse Northern, in which the cloned DNA from the genomic walk was probed with <sup>32</sup>P-labeled cDNA prepared from 0- to 7- and 7- to 12-hour embryos. Hybridizing fragments were then used to probe Northern. The *rpr* gene encodes a ~1.3-kb transcript.
41. A cosmid that overlaps the *rpr* transcription unit was isolated from a genomic library of *iso-1 Drosophila* DNA in the NotBamNot-CoSpeR transformation vector (provided by J. Tamkun). DNA for transformation was prepared with the Qiagen plasmid purification kit. Transformation was carried out as described (35). From 2300 injected embryos a single transformant was obtained. The NT1B1 transgene inserted on the third chromosome and was recombined onto an *H99* chromosome. The transgene was also mobilized by crossing flies to a genomic source of transposase [ $\Delta 2-3$ , 99B; H. M. Robertson *et al.*, *Genetics* 118, 461 (1988)]. Insertions on the second chromosome were recovered, and lines were constructed which contained four copies of the transgene in an *H99/TM3* background.
42. TUNEL was carried out essentially as described (32), with modifications as suggested by S. Robinow (University of Washington). The embryos were fixed for 30 minutes in 4 percent paraformaldehyde and devitellinized as described (6). They were rinsed three times in 1 × phosphate-buffered saline (PBS) containing 0.3 percent Triton X-100, and once in 1 × terminal transferase buffer [Boehringer Mannheim Biochimica (BMB)] (2.5 mM CoCl<sub>2</sub>, 0.3 percent Triton X-100). The embryos were incubated for 3 hours at 37°C in reaction buffer, which consisted of 1 × terminal transferase buffer [2.5 mM CoCl<sub>2</sub>, 0.3 percent Triton X-100, terminal transferase (0.5 U/ $\mu$ l)], 10  $\mu$ M dUTP consisting of a 1:2 mix of Bio-16-dUTP (BMB) and dUTP (BMB)]. Embryos were washed for 1 hour in 1 × PBS containing 0.3 percent Triton X-100. The biotinylated nucleotides were visualized with fluorescein isothiocyanate (FITC)-avidin DN (Vector), incubating for 1 hour in 1:200 dilution, and then washing. Alternatively the Vectastain kit was used as described (6). Fluorescent signals were imaged on the confocal microscope.
43. We used two degenerate oligonucleotide primers (HS#1: ATG-GCN-GTG-GCN-TTC-TA[C/T]-AT, HS#3: CC-GGT-CTT-NGG-[A/G]TG-[A/G]CA), corresponding to amino acids 1 to 7 and 49 to 54 for PCR amplification of a 160-bp DNA fragment from *D. simulans* genomic DNA. This PCR product was directly sequenced with <sup>32</sup>P end-labeled primers.
44. In situ hybridizations were performed [D. Tautz and C. Pfeifle, *Chromosoma* 98, 81 (1989)], with the use of single-stranded RNA probe labeled with digoxigenin, according to a protocol communicated to us by R. Bodmer (University of Michigan). This probe was generated from the 900-bp 13B2 cDNA clone. The observed pattern of transcription was specific to antisense probes, and was absent in *H99* embryos.
45. Double labelings were done with the use of three different protocols. For Fig. 9A, the embryos were labeled by TUNEL, washed after the terminal transferase reaction step, dehydrated, and taken through the in situ protocol as described above. Embryos were incubated overnight at 4°C with absorbed FITC-conjugated antibody to digoxigenin (BMB), and diluted 1:40. Embryos were washed and incubated for 1 hour at room temperature with Texas Red-conjugated avidin (Vector) and diluted 1:200. After further washing of the preparation, the signals were visualized by confocal microscopy. For (B), the entire in situ protocol was carried out first, with the use of an alkaline phosphatase antidigoxigenin antibody (BMB). After the histochemical reaction to detect alkaline phosphatase, the TUNEL reaction was carried out. FITC-avidin was used to visualize the dying cells. Imaging was done on a confocal microscope. For (C), the entire TUNEL protocol was carried out first, with the use of a horseradish peroxidase-conjugated avidin. After the peroxidase reaction, the embryos were washed and dehydrated, and the in situ reaction was carried out with the alkaline phosphatase antidigoxigenin antibody. This third technique provided the best sense of the extensive overlap between cell death and *rpr* expression, but did not photograph well.
46. J. M. Abrams and H. Steller, in preparation.
47. We thank M. Abbott for alleles of *head involution defective*; W. A. Segraves for cloned DNA in the 75C1,2 region; J. Tamkun for the NotBamNot-CoSpeR *Drosophila* cosmid library; R. Davis for the *Drosophila* genomic lambda library; G. M. Rubin for the *Drosophila* eye disc library; J. W. Truman for suggesting the elf-1 antibody to mark persistent neuroblasts; D. Schmucker for the initial observation of extra Kr expressing cells in *Df(3L)WR4* embryos; R. Bodmer for the in situ protocol with RNA probes; S. Robinow for suggestions on the TUNEL protocol; D. Vu and M. Rivera for assistance in generating new deletions; and H. R. Horvitz for comments on an earlier version of this manuscript. Supported in part by a Pew Scholars Award (H.S.), an NIH postdoctoral fellowship 5 F32 NS08536 (K.W.), a postdoctoral fellowship from the American Cancer Society. K.W. and J.M.A. were postdoctoral associates, and H.S. is an Associate Investigator with the Howard Hughes Medical Institute.

22 February 1994; accepted 16 March 1994